ingegneria sismica
International Journal of Earthquake Engineering
Anno XLIII - Num. 2 - 2026

Optimization of virtual power plant power peaking considering net load peak-to-valley difference

Zhenhai Zhu[1,*], *Jiye Hu*[2], *Hui Sun*[1], *Yong Guo*[1], *Lang Gan*[1] *and Lei Yang*[1]

[1] Guangdong Power Grid Energy Investment Co., Ltd, Guangzhou, Guangdong, 510200, China

[2] Beijing Chuangzhixinke Science and Technology Co., Ltd., Beijing, 100083, China

SUMMARY: *About the growing gap between the peak and trough values of the net load in the new-energy grid-connected virtual power plant, people have already confirmed that the traditional peak-adjustment optimization method does not have effect. This research puts forward a power peak disposition model for the virtual power plant, which depends on the hierarchical particle swarm optimization algorithm. The core part of this model is constituted by three optimization objectives. Firstly, this object has the purpose of reducing to the smallest extent the electricity costs of users. Second, it makes great efforts to realize the maximum value of the net profit of this system. At last, this paper's goal is to lower the expense of power peak cutting distribution within a fixed time period. When we make the model, practical restrictive conditions are considered by us. These factors include the power balance that is inside the electric power system, the electric energy generation ability of electromechanical devices, and also the climbing capacity. For the solving of the model, the iterative computation capability which is possessed by the layered particle swarm within the hierarchical particle swarm optimization algorithm is utilized by us. By means of a method that is systematic and divided into phases, the most beneficial disposition for the peak load cutting work of the virtual power plant is got decided. This model may obtain an 18.24 percent cut of carbon discharge, and it only lets the cost of power production undergo a 9.56 percent growth. Furthermore, it brings about a notable decrease in the net load peak-valley difference. When make comparison with the strategy of constant power, the strategy which this paper puts forward can completely make use of the constraints of energy storage. This permits the peak scheduling to reach the most superior distribution, hence providing an effective scheme for the safe, cost-cutting, and low-carbon running of the virtual power plant.*

KEYWORDS: *virtual power plant; net load peak-to-valley difference; hierarchical particle swarm optimization algorithm; multi-objective optimization; power peaking optimization*

1 Introduction

With the gradual increase in the penetration rate of green energy such as wind power and photovoltaic in the power grid, renewable energy such as wind power and photovoltaic in the power grid to deliver a large amount of clean power at the same time, by their own output intermittent, fluctuating characteristics, but also to the stable operation of the power system has brought a series of problems [1-3]. In particular, the uncertainty of wind power output, coupled with the existence of load forecasting errors, which leads to the net load peak and valley

*LONGYIN0707@163.com
https://doi.org/10.65102/is2026576 Published: 30 April, 2026

differences in the existence of randomness, increasing the power system peak pressure [4, 5]. For example, the large amount of uncertainty and strong volatility in the power output of renewable energy sources, such as wind power, makes it necessary for the system to prepare more standby units to participate in peaking [6]; in addition, there is a serious temporal mismatch between peak loads and uncertain power sources due to the habits of the production industry as well as the residential power consumption. At the same time, the anti-peaking characteristics of wind power, among others, lead to an increase in the net load peak-to-valley difference [7]. The highest electricity load duration hour in a region was 118.6 hours in 2018, but in order to satisfy this short-lived peak, an investment of nearly 20 billion yuan was needed to upgrade transmission, distribution, and power lines and supporting equipment. Therefore, thus, it has very important practice meaning to study methods for reducing the peak pressure which acts on the electric power grid.

Virtual power plant is a typical cooperative alliance, distributed energy from different subjects can play out the complementary effect between various types of energy by aggregating into virtual power plant and participate in the power market transaction as a whole [8]. Nevertheless, the problem of how to properly distribute the advantages after cooperation is a widely existing issue. Therefore, the academic circle holds that there exist differences in the cost efficiency and output characteristics of different kinds of distributed energy resources.The key point lies in that the reasonable combination of many scattered energy resources, which therefore can make the cooperative and optimized effect of virtual power plants reach the maximum. For example, Jia, Y et al. proposed an economically optimal scheduling method for virtual power plants under time-of-use pricing for electric vehicles based on incentive demand response strategy and dynamic load compensation, which establishes an optimization model for maximizing the economic efficiency of a virtual power plant by taking into account system constraints such as power balancing, new energy outputs from wind and solar, and the operating costs of the storage system, while incorporating time-of-use tariffs [9]. Zhang, F et al. constructed an optimal scheduling model based on stochastic optimization theory aiming to maximize the expected economic benefits of daily operation of a virtual power plant, which is based on the stratified sampling principle of Latin Hypercubic Sampling, and the model generates a scenario sample set of the joint distribution of the scenarios of wind and light outputs, which provides data support for the optimization of scheduling [10]. Guo, W et al, on the other hand, proposed a multi-objective optimization decision-making process which can maximize the comprehensive benefits of the virtual power plant by considering both economic and social benefits in the day-ahead-intraday market to develop a bidding strategy for the virtual power plant [11]. Chen, Y et al. With the goal of achieving carbon neutrality, given the uncertainties in wind, solar and load demand, the study proposes a two-stage robust optimization model that is capable of determining the bidding strategy and the mix of units for a virtual power plant based on the predicted values of wind, solar, and loads, and determining the outputs of each unit by taking into account the set of uncertainties to achieve the best operational efficiency in the worst case scenario [12]. Michael, N E et al. constructed a virtual power plant scheduling model containing electric vehicles, photovoltaics, energy storage systems and data centers to optimize the scheduling scheme to maximize the revenue of the virtual power plant taking into account the fluctuation of the market price of electricity and the uncertainty of the new energy output [13]. Elgamal, A H et al. proposed a Deep Deterministic Policy Gradient (DDPG) model for the operation and management of a virtual power plant considering solar energy, which enters into a Direct Purchase Agreement (PPA) with the grid and supplies both electricity and heat to the consumers to meet the demand when there is a shortage of solar energy, which balances the instability of solar energy and ensures an efficient energy supply [14].

For the purpose of attaining more effective resource allocation, multitudinous scholars have brought demand response schemes into the optimized operation of virtual power plants. For example, Ju, L et al. proposed a data-driven two-phase virtual power plant robust optimal scheduling model (BDCD-VPP) considering the carbon-green certificate equivalence conversion mechanism, which improves the Aumann-Shapley method by incorporating the risk factor, the cost factor, and the carbon-recovery factor, and the model is constructed by using a strong dyadic theorem and the C&CG algorithm [15]. Rahimi, M et al. modeled wind power output, load and market prices using an interval uncertainty approach to optimize a two-stage trading strategy for day-ahead-real-time of the virtual power plant, which resulted in improved profits for the virtual power plant in both markets [16]. Cavazzini, G et al. proposed a techno-economic analysis framework for evaluating the benefits of combining a seawater pumped storage power plant with a wind power plant, using the Adaptive Search Diversified Particle Swarm Optimization (ASD-PSO) algorithm to optimize the virtual plant scheduling plan to maximize the benefits [17]. Tan, Y et al. proposed a multi-objective optimization method for low-carbon economic scheduling of a combined heat and power virtual power plant (CHP-VPP), which comprehensively considers equipment operating characteristics and correlations, and constructs an optimization function through a diverse penalty mechanism in order to maximize profit and minimize carbon emissions [18]. Sharma, H and Mishra, S simulated DER generation and load profiles for 11 kV feeder using DER-CAM model by designing a virtual power plant model to address the problems of backflow, voltage fluctuations and loss of grid revenues that may be caused by high penetration of DER such as solar PV [19]. Zhao, H et al. introduced the carbon trading mechanism into a low-carbon, multi-energy virtual power plant and constructed a novel dynamic robust optimization model considering multiple uncertainties in source-load, which was empirically shown to be effective in reducing the conservatism of robust optimization methods [20].

The grid-connected capability of renewable energy has a steady increasing trend. But, the intermittent property and randomness of renewable electric energy, together with its anti-peak adjustment features, hence will bring about a conflict between power generation resources and electric loads inside the electric grid. This greatly limits the electric grid's capability for receiving renewable energy. Therefore, researchers put their focus on reducing wind power changes, carrying out economic and technology evaluations, doing peak cutting and valley filling, and improving power supply dependability. Their goal is to let the mutual make up for each other of the merits of different resource kinds and promote the use efficiency of clean dispersed energy. For example, Lee, S J et al. designed a cooperative control optimization algorithm based on master-slave control for distributed energy storage power plants, which realized the coordinated operation of distributed energy storage power plants between peak and frequency regulation, although the cooperative operation of multiple storage power plants was considered without improving the utilization rate of a single storage power plant [21]. Ning, Y et al. developed a mathematical optimization model of peak load shifting for microgrid battery energy storage system, which uses an islanded microgrid for simulation and analysis, and solves the model and obtains the BESS power for each dispatch cycle through the interior point method to achieve the optimal operation of the BESS and the purpose of peak shaving and valley filling in microgrids [22]. Banshwar, A et al. proposed a market-based approach that allows renewable energy producers to participate in day-ahead market clearing of energy and ancillary services in a decentralized framework that utilizes optimal tidal current techniques to sequentially clear the energy market and ancillary services market in order to minimize the procurement cost and obtain a viable solution [23]. Liu, S et al. proposed a hybrid control strategy based on state-of-charge (SOC) optimization for FM and FD of energy storage system to achieve cooperative operation of energy storage in FM and FD scenarios based on the SOC state of the energy

storage system, which improves the utilization rate of energy storage resources [24].

Furthermore, Badesa, L et al. proposed a time-ordered operation simulation (COS) based model combined with a time-domain decomposition based computational load balancing technique in order to analyze the validity of the long-term impacts of the peaking ancillary services market (PRSM) in China's power system as well as its necessity and cost-effectiveness in the adaptation of renewable energy sources [25]. Li, H et al. proposed a two-stage synergistic optimization model of pumped storage and all-vanadium redox flow battery (VRB-PS) comprising a HESS, where the VRB can suppress high-frequency fluctuation of wind power and the PS can improve the utilization of wind power, and this HESS has a better regulating capability and operating economy [26]. Heydari, R et al. mentioned that the Etelligence project centrally regulates a wide range of distributed generation facilities and loads by implementing strategies such as time-of-day tariffs, real-time tariffs, and peak-to-valley tariffs, which enhances the uptake of renewable energy sources and promotes synergism between supply and demand for electricity by controlling dispatchable loads [27]. Cui, Z et al. proposed a two-layer stochastic optimal dispatch model to cope with the double uncertainty of wind power output and load demand, the upper model pursues the minimization of power generation cost, and the lower model optimizes the standby allocation and renewable energy dispatch through the CVaR risk metrics, this architectural design improves the system operation reliability while ensuring the economy through risk-aware decision-making mechanism [28]. Liu, J et al. The aim of the proposed scheduling strategy is to achieve the best peaking effect at the lowest cost, considering various factors such as charging and discharging constraints of SOC, capacity constraints of EV and BESS, time-of-use tariffs (TOU), etc., which are solved by using the improved MOPSO algorithm [29]. All the above-mentioned literatures only carry out examination on the effect of peak cutting and valley filling from either an economic angle or a control angle. Furthermore, the optimization schemes are established on the basis of forecasted certain digital magnitudes. When great differences appear in the forecast results of wind energy power, solar panel power, or load, the actual optimized outcomes may depart from the ideal optimum solution. Only a restricted quantity of research works have analyzed the demand, the expense, and the peak cutting effect of energy storage in the background of the real electric power grid.

In this research paper, we at first begin to make a mathematical description of the scattered power sources, demand-side properties, and energy storage devices inside virtual power plants. The present analysis is conducted by this paper from two aspects which are power supply and power demand of virtual power plants. By means of this process, we have successfully constructed a comprehensive model about virtual power plants, which acts as the cornerstone for the exploration of the optimal distribution of resources in virtual power plants that are used for electric power peak shaving.Next, we establish a mathematical model which is used for multi-objective optimization. The objectives of this model's scheme include economic efficiency, environmental protection, and expenditures related to peak-load cutting down.For the solving of this model, we have introduced a hierarchical particle swarm optimization algorithm. By utilizing its layered repeated working principle, we are able to reach cooperative question handling, hence allowing the adjusted arrangement of manifold resources inside the fictitious power station. For the purpose of verifying the effect of the method we put forward, we have designed simulation experiments. These experiments have the purpose to evaluate the peak-cutting influence of the model from many different aspects. In addition, we carry out the comparison between the peak-cutting outcomes gotten by our method and the outcomes gotten by a fixed-power strategy, which gives a comprehensive assessment of the effect of our put-forward solution.

2 Hierarchical particle swarm optimization algorithm based virtual power plant peaking optimization

2.1 Mathematical model of virtual power plant

2.1.1 Distributed Power Modeling

In photovoltaic power generation, the light intensity in a certain area changes with time as a random variable, and currently the Beta distribution has been adopted by most scholars and researchers to simulate the stochastic distribution characteristics of light intensity, and a large number of studies have proved its effectiveness and accuracy. Therefore, the photovoltaic system's output may be considered as a variable which obeys the Beta distribution. Therefore, the probability density of photovoltaic output may be obtained in the form shown below:

$$f\left(P_t^{PV}\right)=\frac{1}{B\left(m_t,n_t\right)}\cdot\left(\frac{P_t^{PV}}{P_{\max}^{PV}}\right)^{m_t-1}\cdot\left(1-\frac{P_t^{PV}}{P_{\max}^{PV}}\right)^{n_t-1} \tag{1}$$

$$B(m,n_t)=\frac{\Gamma(m_t)\cdot\Gamma(n_t)}{\Gamma(m_t)+\Gamma(n_t)} \tag{2}$$

$$m_t=\mu_t^{PV}\cdot\left(\frac{\mu_t^{PV}\cdot\left(1-\mu_t^{PV}\right)}{\sigma_t^{2,PV}}-1\right) \tag{3}$$

$$n_t=\left(1-\mu_t^{PV}\right)\cdot\left(\frac{\mu_t^{PV}\cdot\left(1-\mu_t^{PV}\right)}{\sigma_t^{2,PV}}-1\right) \tag{4}$$

where $B(m,n)$ represents the Beta distribution function of solar radiation, m and n represent the corresponding Beta distribution parameters; P_t^{PV} is the predicted value of PV in t time period; μ is the mean value of solar radiation; σ is the variance of solar radiation.

Just the same as solar electric production, wind electric production in basic nature is a kind of electricity source that has intermittent character, and its output is affected by the wind speed, which shows a strong randomness. Compared with photovoltaic power generation, its prediction accuracy is lower and the error is larger, but different wind farms in different geographic locations or different units of the same wind farm, because of the many different geographical locations and air flows, its output can, on a certain degree, form a complementary relation.

Because different wind power fields and many wind turbine generators (WTGs) inside the same wind power field have complementary characteristics of power output, therefore the degree of power output fluctuation increases in the order of two wind power fields, one single wind power field, and one single WTG.In the field of wind electricity produce, wind speed is a random change quantity. Quite many scholars hold the viewpoint that its randomness obeys the Weibull distribution. Furthermore, multitudinous literature researches have verified its validity and accuracy, hence this distribution is utilized in the great majority of areas. Because the output quantity of wind energy power generation is connected with wind speed, the probability density function of wind energy output can be given in the following way:

$$f\left(P_t^{WT}\right)=\frac{k_t}{l_t}\cdot\left(\frac{P_t^{WT}}{l_t}\right)^{k_t-1}\cdot e^{-\left(\frac{P_t^{WT}}{l_t}\right)^{k_t}} \tag{5}$$

where k and l are the scale and shape parameters of the Weibull distribution, respectively.

Beyond solar and wind energy, very many countries and regions have also accepted various kinds of renewable energy electricity generation, including biogas-based electric power production and geothermal electric power generation, tidal power generation, etc. These forms of power generation are not as widely noticed as solar and wind power, and their development process is also relatively slow.

2.1.2 Demand-side resource modeling

Beside gathering together flexible and changeable scattered resources on the generation side, virtual power plants also can indirectly achieve the result of promoting the generation-side power output through controlling adjustable loads. Adjustable load resources, which are constituted by transferable load resources and interruptible load resources, are acting as effective methods to resolve the power generation gap and push forward the continuous development of energy.

Transferable loads and interruptible loads essentially belong to the price-type and incentive-type of demand response, respectively. Price-based refers to the behaviors of consumers that change their electricity use patterns according to time-of-use electricity price standards, which mainly include the following three kinds: time-sharing tariffs for different time periods in terms of years, months or days; real-time tariffs for different time periods at hourly or minute levels; and peak tariffs for adding peak hours on top of the real-time tariffs. According to the time-based pricing system, consumers have the capability to shift a part of their electricity consumption among different time periods. Therefore, they are able to reduce the expenditures which are connected with the using of electric power.

Incentive type belongs to a frame which, according to the whole supply-demand situation of the electric system, cuts down part of the load when power is lacking, and gives users price encourage either direct or indirect way. This category includes direct load control work, interruptible load arrangement works, demand-side bid inviting, and emergency demand response, among other items.

The following are modeled for transferable load and interruptible load respectively.

(1) Transferable load model

The model of load that can be transferred has the ability to realize peak cutting and valley filling. It achieves this work through the setting of tariff levels for peak time periods, low-demand time periods, and normal work days. Afterwards, it causes users to move a part of their load from peak time frames to time segments of low requirement and ordinary work days. The model of transferable load is given in what follows:

$$D_t=d_t+d_{t,up}-d_{t,down} \tag{6}$$

where D_t characterizes the value of load demand at time t after the time-of-day tariff incentive is applied; d_t characterizes the value of load demand in hour t before the time-of-day tariff incentive is conducted; $d_{t,up}$ characterizes the increase in load in hour t; $d_{t,down}$ characterizes the reduction of load in time period t, and $d_{t,up}$ and $d_{t,down}$ are mutually exclusive in time period t and the total amount of load remains constant throughout the scheduling cycle, i.e:

$$\begin{cases} d_{t,up} \cdot d_{t,down} = 0 \\ \sum_t d_{t,up} = \sum_t d_{t,down} \end{cases} \tag{7}$$

The constraints on $d_{t,up}$ and $d_{t,down}$ are as follows:

$$B_{t,up} \cdot d_t \geq d_{t,up} \geq \varepsilon_{up} \cdot d_t \cdot \left(1 - \frac{Pr_t}{Pr_{ref}}\right) \tag{8}$$

$$B_{t,down} \cdot d_t \geq d_{t,down} \geq \varepsilon_{down} \cdot d_t \cdot \left(\frac{Pr_t}{Pr_{ref}} - 1\right) \tag{9}$$

where $B_{t,up}$ characterizes the maximum increase in the weight of the load at time t and $B_{t,down}$ characterizes the maximum decrease in the weight of the load at time t; Pr_t characterizes the actual electricity price in time period t and Pr_{ref} characterizes the reference electricity price in time period t; ε_{up} and ε_{down} characterize the elasticity coefficients of load increase and load decrease with respect to electricity prices, respectively.

(2) Interruptible Load Model

The interruptible load model promotes the grid's reserve resources through cutting a part of the load in peak time periods. Therefore, it has realized the optimal distribution of resources in the interior of the power grid. The model of interruptible load includes the model of compensation capacity cost and the model of interruption capacity cost. Under this circumstance, the compensation ability shows the amount of interruptible load, and the compensation ability cost model is given in the following way:

$$C_{t,j}^C = \beta_{t,j} \cdot Q_{t,j}^C \tag{10}$$

where $C_{t,j}^C$ denotes the compensated capacity cost for t time period, $Q_{t,j}^C$ denotes the compensated capacity for t time period, and $\beta_{t,j}$ denotes the compensated tariff for t time period.

Interruptible Capacity represents the amount of load that is actually interrupted and is modeled as follows:

$$C_{t,j}^H = \gamma_{t,j} \cdot Q_{t,j}^H \tag{11}$$

where $C_{t,j}^H$ denotes the interruptible capacity charge for time period t, $Q_{t,j}^H$ denotes the interruptible capacity for time period t, and $\gamma_{t,j}$ denotes the interruptible tariff for time period t.

2.1.3 Energy storage system modeling

In the inside of virtual power plant, the electric power which comes from wind and solar energy resources has the properties of randomness and intermittency. Furthermore, the electric power consumption of different load categories also cannot be predicted. As the connection which lies between the power generation side and the power consumption side, the energy storage unit

possesses very great significance. This facility can effectively weaken power fluctuations, realize peak cutting and valley filling inside the virtual power plant, thus making the system be able to keep a condition of dynamic balance.

Below is the model that is used for computing the charge condition of the energy storage component in the battery's discharging time period:

$$SOC_t = SOC_0 - \eta_d \frac{I_d \Delta t}{C} \tag{12}$$

where SOC_0 denotes the initial charging state of the battery, SOC_t denotes the charging state of the battery after the discharging Δt time, I_d denotes the discharging current, η_d denotes the discharging efficiency, and C denotes the total power of the battery.

In the time that battery carries out charging, the estimate model for the charge condition (SOC) of the energy storage unit is given below:

$$SOC_t = SOC_0 + \eta_c \frac{I_c \Delta t}{C} \tag{13}$$

where I_c denotes the charging current and η_c denotes the charging efficiency.

2.2 Load Peak-to-Valley Difference and its Derived Indicators

The difference between the tallest and shortest points of load need, which is called the peak-valley change of load demand, is the gap between the biggest and smallest levels of load demand inside a certain region during one whole day.It is used for showing the degree of changes in the load need on that day. A bigger numerical value therefore indicates a more notable extent of change of the load demand on this day and a higher degree of difficulty for grid peak-shaving work. The expression is written just below:

$$P_i = P_{i,\max} - P_{i,\min} \tag{14}$$

where: P_i is the peak-to-valley load demand difference of a regional grid on day i; $P_{i,\max}$, $P_{i,\min}$ are the extreme value and the minimum value of the load demand of a regional grid on day i, respectively.

For more accurately describe the distribution condition of the peak-valley gap in load requirement inside one area, a computation method is often used by people to get the calculated values of the peak-valley gap (such as maximum values, mean values, standard variances, and probability distribution situations). After that, this makes possible a more accurate evaluation of the peak problem which the regional electric power grid faces. This evaluation is established upon the distribution of the gap between peak and trough numerical values and the changes in load demand conditions.

2.2.1 Load Demand Peak and Valley Difference Extremes

The most extreme instances of the gap between peak and trough in load demand represent the most difficult and the least difficult situations regarding the peak-trough gap of the regional electric power grid. To speak more concretely, the largest digit values of the peak-valley gap reflect the most difficult conditions for the regional power grid’s peak-valley management work, while the smallest digit values reflect the least difficult ones. Below we give the expression

which has relation to this content:

$$P_{\max} = \max\left(P_i\right) \tag{15}$$

$$P_{\min} = \min\left(P_i\right) \tag{16}$$

where: $P_{\max}$, $P_{\min}$ are the maximum and minimum values of the peak-to-valley difference of load demand in a certain period of time in a regional power grid, respectively.

2.2.2 Average peak-to-valley difference in load demand

The mean difference between the maximum and minimum numerical values of load demand describes a whole condition concerning the difficulties that are encountered in grid peak cutting within this region. We here present it in the following manner:

$$P_{mean} = \frac{1}{n}\sum_{i=1}^{n} P_i \tag{17}$$

where: P_{mean} is the mean value of the peak-to-valley difference of load demand in a certain period of time in a regional grid; n is the total number of load sampling points in a certain period of time in a regional grid.

2.2.3 Standard deviation of peak and valley differences in load demand

The standard difference of the gap between the maximum and minimum numerical values of the load requirement describes the changing condition which is connected to the problem of peak cutting for the electric grid inside this region. At this place, we show it in the below method:

$$P_{stdev} = \sqrt{\frac{1}{n}\sum_{i=1}^{n}\left(P_i - P_{mean}\right)^2} \tag{18}$$

where: P_{stdev} is the standard deviation value of the peak-to-valley difference in load demand for a certain period of time in a regional grid.

2.2.4 Probability distribution of peak-to-valley differences in load demand

The probability distribution of the interval between the maximal and minimal points in load demand is utilized by us to describe the numerical dispersion of this peak-valley difference. According to this probability distribution, the cumulative probability distribution of the peak-valley difference of load demand is usually got through this method. The formula of it is as what follows:

$$f\left(P_V\right) = \frac{1}{n} num\left(P_V\right) \tag{19}$$

$$F\left(P_V\right) = sum\left[\, f\left(P_{Vj}\right)\right] \tag{20}$$

where: P_V is the data in the set of load demand peak-valley difference; P_{Vj} is the j th data

in the set of load demand peak-valley difference less than P_V; $num(\cdot)$ is the frequency of occurrence of a certain number in the set of data; $sum(\cdot)$ is the summation function; $f(\cdot)$ is the probability distribution function; $F(\cdot)$ is the cumulative probability distribution function.

According to the cumulative probability distribution of the peak-to-trough gap of load demand, the probability that the peak-to-trough gap of load in this region exceeds the peak-shifting difficulty threshold is ascertained. This probability is utilized to comprehensively portray the difficulty of peak movement of the region within a determined time scope. The peak-shifting difficulty threshold is usually established by regional scheduling persons according to the local peak-shifting condition and their arrangement experience. This method can be utilized when the area's new-energy power generating cannot get full utilization. In these situations, the peak-to-trough difference of the load demand which can be temporarily absorbed by means of inter-regional spot trading is utilized to realize consumption.

2.3 Impact of virtual power plant on grid load profile

We may take the real-time load curve of G province power grid on July 8, 2022, as one example, therefore to discuss the anti-peaking problem of virtual power plants. Figure 1 gives out the distribution load and net load curve of the whole network for that one day. This result shows that when we consider the influence of new energy output on the load, because of the anti-peaking property which new energy has, the gap between peak and valley that conventional power sources and in-province out-of-region power receivers need to bear has got larger. To speak specifically, this number has been increased from 10.45 million kilowatts (MW) to 14.6 million kilowatts (MW). In addition, the depth of the low-valley peak has gotten a further reduction, falling from 61.8 million kilowatts (MW) to 56.5 million kilowatts (MW). This condition puts forward more strict requirements on the peak-adjustment ability of traditional energy suppliers and cross-region power receivers. Therefore, more strict requirements have been put forward for the peak-cutting abilities of these units.

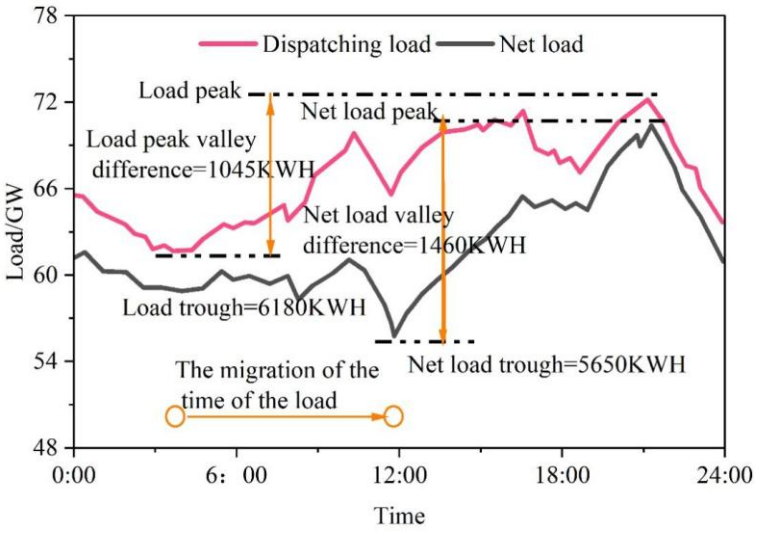

Figure 1: The effect of virtual power plant on the daily load curve of the grid

Furthermore, under the influence of the new energy output, the time point of the power grid's net load trough which is shown in Figure 1 has obviously shifted from 3:55, that is the time point of the dispatch load trough, to 11:50. In addition, more detailed statistical works have been carried out on the time distribution of the dispatch load trough time points and the net load

trough time points in the whole year of Province G. The result situations of the distribution of the dispatch load trough time points and the time distribution of the net load trough time points are shown in Figure 2 and Figure 3 separately.

Obviously, the new energy output that comes from the virtual power plant not only can further decrease the power grid's minimum load level and expand the peak-valley difference but also has the possibility to bring about an offset when the system is in the load trough period. Therefore, the load performance features of the electric power network have had great changes happen. Along with the unceasing growth of the installed quantity of new energy, the influence of new energy upon the power grid's load trough and its peak-valley gap shall be further enlarged. Therefore, the contradiction which exists in peak load management of the power grid will become more prominent.

And the existing new energy on the grid peak impact study, generally only for scheduling load trough moment to carry out. After the large-scale new energy grid, the new energy output may lead to the net load trough moment and scheduling load trough moment deviation, only the study of scheduling load trough moment of virtual power plant new energy output on the grid peaking impact results are too optimistic.

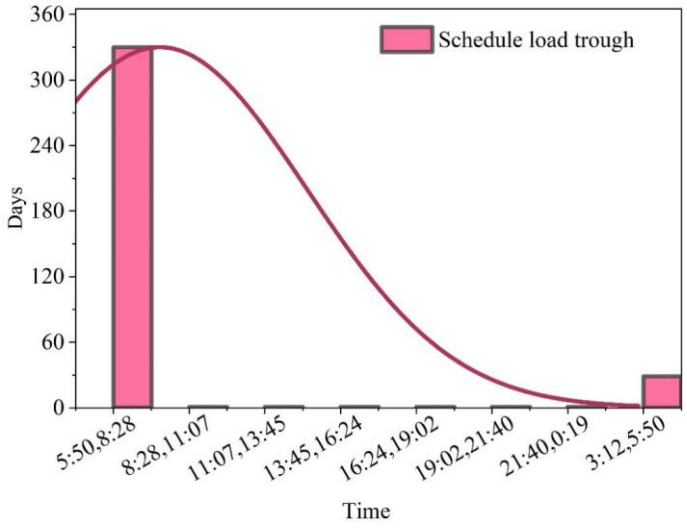

Figure 2: Distribution of scheduling load trough

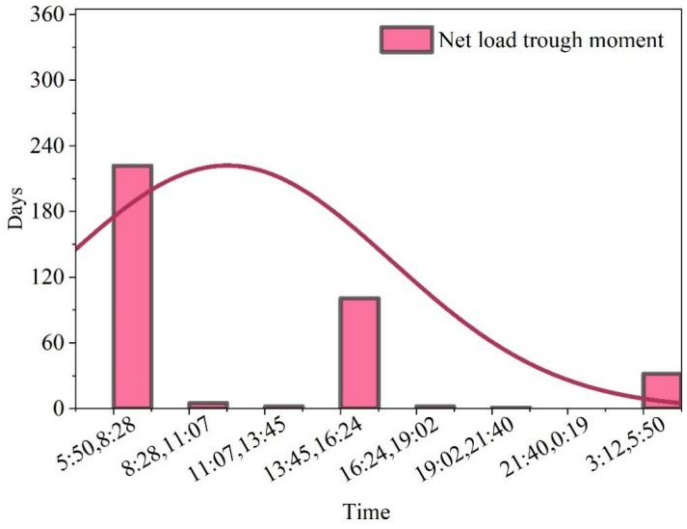

Figure 3: Net load trough moment

2.4 Virtual power plant peaking configuration model design

The grading-type particle swarm optimization algorithm is utilized as the optimized disposition algorithm for electric power system peak load adjustment. To those users whose measurement instruments cannot satisfy the standard of 24-hour signal collection, a virtual power plant peak-shifting configuration model is established by us. The objective function which belongs to the virtual power plant peaking configuration is formulated by us. The objectives are to make the user's electricity spending as small as possible, make the system's net income as large as possible, and make the peaking cost in the whole power supply cycle as small as possible. When we carry out the consideration of the common work situations of the electric power system, constraint conditions are set up for the peak-adjustment distribution of the virtual power plant. After that, the hierarchical particle swarm optimization algorithm is used by us to look for the optimal solution of the objective function in these constraint conditions. By means of this procedure, the most advantageous peak-cutting arrangement scheme for the virtual power plant can be gotten.

2.4.1 Mathematical expression of the objective function

The goal function is a key important component in the virtual power plant power peak adjusting configuration model. This model is established in accordance with the demands of virtual power plant electric power peak-clipping configuration. Its targets are to cut down the user's electricity expenditure to the most low possible level, make the system's net income become maximum, hence reduce the total peak-shaving expenditure on continuous time intervals to the minimum. When we consider the user's basic electric charge and the electric cost in peak time inside the charging cycle, the sub-target function which is used to lower the user's electric spending to the smallest level is:

$$\min f_1 = \max c + \max p + p_* \cdot \sum_{i=1} Wt \tag{21}$$

where $\min f_1$ is the user cost minimization sub-objective function; c is the peak hour electricity cost in the user's daily electricity bill; $\max p$ is the maximum power consumption value in the user's electricity cycle; p_* is the user's basic electricity price; i is the number of electricity load points in the user's electricity cycle; W is the average power of the users in the slot in a single power peaking configuration. .

The peak power configuration is mainly obtained through adjusting the output of the generating units that belong to the power system. It is an unavoidable thing that the adjustment of peak electric power can bring changes to the economic benefits of the electric power system. Therefore, as concerning the sub-goal which gets the biggest net incomes of the system, the target function is just like below:

$$\max f_2 = R + d + C - s\omega \tag{22}$$

In the formula, $\max f_2$ is the sub-objective function of maximizing the net benefit of the system; R is the coal saving benefit of the power system; d is the benefit of reducing the generating unit's output of the power system; C is the compensatory benefit of the power system's peaking; s is the conversion factor of the investment in the power system; and ω is the daily operation and maintenance cost of the power system.

The third secondary objective carries the purpose of cutting down the total peak cost that exists over continuous time periods. The function which corresponds to this second target is

just like below:

$$\min f_3 = \sum_{t=1} a_t K_{je} + \sum_{N=1} b_N L \tag{23}$$

where $\min f_3$ is the objective function to minimize the total peaking cost in a continuous period of time; t is the time period; a_t is the virtual power plant peaking offer of any generating unit in the power system in the t th period of time; K_{je} is the e th segment peaking amount of the generating unit of the power system in the j th period of time; j is the number of the regular generating units in the power system; N is the number of generating units with load regulation conditions in the power system; b_N is the power peaking offer of the N th adjustable load body in the power system in a certain time period; and L is the power peaking amount of generating units with load mediation conditions in any time period.

For the purpose of simplifying the calculation which comes after, the three above-mentioned sub-objective functions are combined into one objective function, that is:

$$f = \min f_1 + \max f_2 + \min f_3 \tag{24}$$

where f is the objective function of the virtual power plant electrical energy peaking configuration.

This objective function synthesizes the three sub-objectives, and the above final objective is subsequently achieved by solving the objective function.

2.4.2 Constraint design

In the process of realizing the peak configuration of electric energy inside the virtual power plant, the power system operation constraints need to be considered to constrain its power balance, output and creep. Among them, the constraints on power system power balance are:

$$P_0(t) + P_*(t) + P(t) = P_{load}(t) + P_{link}(t) \tag{25}$$

where $P_0(t)$ is the power generation of conventional generating units in the power system at the t moment; $P_*(t)$ is the power generation of wind turbines or thermal power units in the power system at the t moment; $P(t)$ is the power generation of energy storage units in the power system at the t moment; $P_{\text{load}}(t)$ is the outgoing power of the power system at the t moment $P_{link}(t)$ is the load value of the power system at the moment of t.

The electric energy output of the generating units which are inside the power system must lie within a specific scope and must not exceed either the upper limit or the lower limit. Hence, the constraint may be described in the following way:

$$\min D \le D \le \max D \tag{26}$$

where $\min D$ is the minimum generation capacity of a generating unit of a power system at any point in time; D is the generation capacity of a generating unit of a power system at any point in time; and $\max D$ is the maximum generation capacity of a generating unit of a power system at any point in time. Climbing constraints on the power system generating units are:

$$-Q_{\max} \le P_G(t) - P_G(t-1) \le Q_{\max} \tag{27}$$

where $-Q_{\max}$ is the maximum climbing rate of any one generating unit in the power system; $P_G(t)$ is the actual power generation in the power system generating unit in the power-on state at the moment of t; $P_G(t-1)$ is the output of the generating unit in the power system generating unit in the power-on state at the moment of $t-1$; $Q_{\max}$ is the maximum climbing rate of any generating unit in the power system.

The above three constraints are used to constrain the virtual power plant peaking configuration.

2.4.3 Hierarchical particle swarm optimization algorithm based power peaking allocation

The objective function which follows the constraints can provide very many solutions. A great number of power peak adjustment arrangement schemes exist which can satisfy both the objective function and the constraint conditions.Therefore, according to the actual demands, hierarchical particle swarms must be carried out by us. Through carrying out repeated level-by-level calculations with this algorithm, the optimal configuration method can be obtained, therefore realizing the optimization of power peaking arrangement.The virtual power plant power peaking configuration model built is shown in Figure 4.

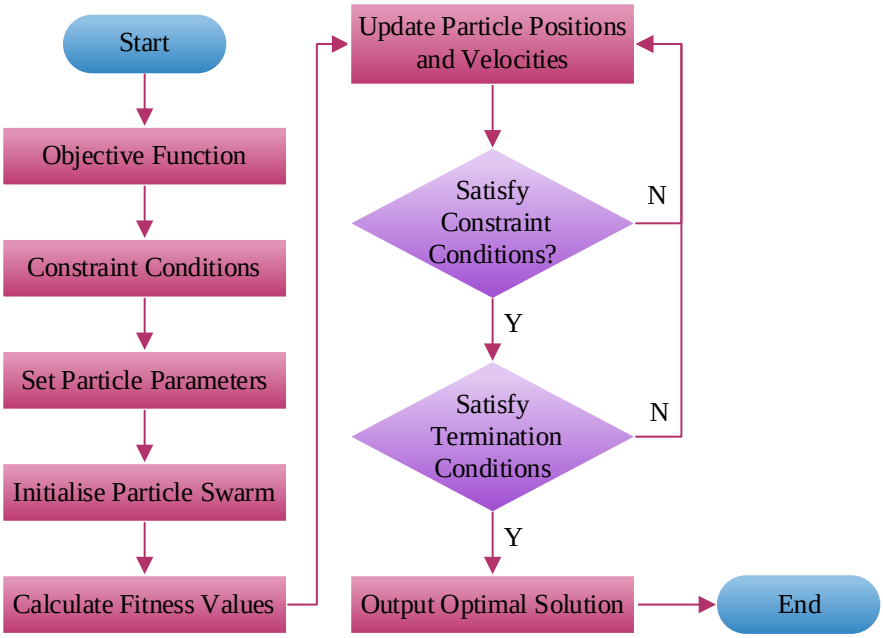

Figure 4: The virtual power plant energy modulation peak configuration model

The step method for utilizing the layered particle swarm optimization algorithm to solve the target function is elaborated as follows.

Step 1: Set particle parameters. Set any one solution of the objective function as a particle α, the number of particles is ν, ν particles to form a particle swarm, which will be placed in a k-dimensional search space with particle size μ.

Step 2:The procedure of establishing individual tiny particles inside the searching region. The initialization includes initializing the search position of individual particles to the origin and initializing the particle search speed η to zero.

Step 3: Carry out the computation of the fitness function. The fitness value expresses the distance that is between the particle's position and the optimal position, and its calculation

formula is:

$$\rho = \sum \left(X_f - x \right) y \tag{28}$$

where ρ is the particle fitness; X_f is the optimal position corresponding to the objective function in the ideal case; x is the farthest moving position of the particle; y is the fitness parameter, which normally takes the value of 0.1.

Step 4:Particle swarm improving change. The particulate matters carry out a searching procedure inside the n-dimensional searching exploration space. Therefore, both the position and the velocity of the particles will have changes occur. According to the fitness degree of the particles, their velocity and position are carried out the update by us. The formula which is used for this update is what follows:

$$\begin{cases} \kappa(t+1) = \tilde{\omega} \times \kappa(t) \times (\zeta - \varphi) + \xi \times \rho \\ \varphi(t+1) = \zeta + \kappa(t+1) \end{cases} \tag{29}$$

where $\kappa(t+1)$ is the particle velocity at the moment $t+1$; $\tilde{\omega}$ is the inertia weight; $\kappa(t)$ is the particle velocity at t moment; ζ is the farthest position of the particle in the search process, i.e. the position with the closest distance to the optimal target; φ is the particle position at t moment; ξ is the weight coefficient; $\varphi(t+1)$ is the particle position at $t+1$ moment.

Step 5: Particle inspection. After each update to output the farthest particle, the corresponding virtual power plant peak power optimization allocation strategy and the constraints against the constraints, if the constraints are met, it will be listed in the list of optimal particles; and then the next update of the particle inspection, if the particle also meets the constraints, the particle position will be compared with the list; if more than the list of particles on the list, it will be replaced with the particle on the list. Repeat the above process until all particles have been inspected, at which time the termination conditions are met, and the particles on the list are output, and their corresponding virtual power plant peaking configuration policy is the optimal policy output, according to which the virtual power plant peaking configuration is realized.

3 Analysis of examples

3.1 Raw data for the algorithm

One simulation system has been built through the use of a five-machine arrangement. This system is constituted by five thermoelectricity generating units, one unified wind power field, and one energy memory system. The wind electricity field could be the mixture of one or more units. In the same way, the energy storage system can possibly be a combining thing of one or more storage battery units. The energy consume and carbon discharge parameters of every unit, together with other parameters of the thermal units, are given one by one in Table 1 and Table 2 separately. The parameters belonging to the energy storage system are displayed in Table 3. We take the dispatch cycle as one day, which is separated into 24 time sections. The installed capability of the wind electric power is 150 megawatts. The parameters which are related with wind turbine and wind speed are detailed in Table 4. The capability of the energy storage device constitutes 60 percent of the capability of the wind power machine. The system load need from

the yesterday is given inside Table 5.

Table 1: Energy consumption parameters and carbon emission parameters

Unit number	a($*(MWH)$^{-2}$)	b($*(MWH)$^{-1}$)	c/$	α(t*(MWH)$^{-2}$)	β(t*(MWH)$^{-1}$)	γ/t
1	0.0732	46.75	1275	$6.755*10^{-6}$	$-5.773*10^{-6}$	$4.256*10^{-6}$
2	0.0911	63.33	2120	$5.855*10^{-6}$	$-6.664*10^{-6}$	$2.651*10^{-6}$
3	0.0495	29.68	2935	$4.769*10^{-6}$	$-5.275*10^{-6}$	$4.425*10^{-6}$
4	0.0633	55.06	1275	$3.512*10^{-6}$	$-3.687*10^{-6}$	$5.536*10^{-6}$
5	0.0506	50.89	2120	$4.769*10^{-6}$	$-5.275*10^{-6}$	$4.425*10^{-6}$

Table 2: Other parameters of the fire crew

Unit number	RU/MW	RD/MW	$T_{ON\ min}$/t	$T_{OFF\ min}$/t	S/$	D/$	P_{MAX}/MW	P_{MIN}/MW
1	56	56	3	3	172	52	220	80
2	32	36	3	3	145	32	110	50
3	165	165	3	3	266	84	620	250
4	65	65	3	3	184	50	350	120
5	65	75	3	3	183	48	350	85

Table 3: Energy storage system parameters

Storage capacity limit (MW.h)	Lower limit of storage capacity (MW.h)	Maximum charge and discharge power (MW)	Charging efficiency	Discharge efficiency	Self-discharge coefficient
250	12	45	0.912	0.948	0.000411

Table 4: Wind turbines and wind speed parameters

Parameter	Numerical value	Parameter	Numerical value	Parameter	Numerical value
P_{wr}/MW	11	v_{ci}/(m/s)	8	k	2.3
v_r(m/s)	19	v_{co}/(m/s)	25	c/(m/s)	12

Table 5: Current system load demand

Time/h	Load/MW	Time/h	Load/MW
1	663	13	932
2	620	14	920
3	594	15	915
4	582	16	919
5	590	17	978
6	613	18	985
7	735	19	982
8	822	20	941
9	934	21	895
10	948	22	818
11	945	23	720
12	932	24	623

3.2 Optimization results and analysis

For the purpose of proving the effect of the model which is put forward in this paper, two simulation situations are assumed by us to assess and study the effect that the energy storage system has on carbon discharge and unit combination costs. Scenario 1 includes one low-carbon economy double-goal model which has not been considered with the net peak-valley difference. By comparison, Scenario 2 is one low-carbon economic double-goal model which has considered the net peak-valley gap. These two scenarios all use the hierarchical particle swarm optimization algorithm to carry out simulation on commercial mathematical software. The parameters of this algorithm have been configured according to the detailed description in Table 6, and the maximum value of evolutionary generations for this algorithm is set as 600.

Table 6: Algorithm parameter setting

Non-dominant proportion	Population scale	Maximum evolutionary algebra	Stop algebra	The fitness function is biased	Cross rate	Mutation rate
0.35	160	600	320	0.03	0.8	0.002

The solution obtained by the model produces a Pareto solution set boundary that lies between the objective of power generation cost and the objective of low carbon. This boundary of Pareto solution set is shown by Figure 5. In the boundary of Pareto solution set, every triangle stands for a set of non-dominated solutions, these are in substance a group of feasible unit output situations. In this figure, the non-dominated solutions have an inversely proportional and uniform distribution which is displayed. This indicates that the model which this paper puts forward uses the hierarchical particle swarm optimization algorithm, that possesses outstanding solution abilities. Furthermore, from this figure, we can see that the Pareto boundary between the power generation cost goal and the low-carbon goal very much looks like an inverse proportion function curve. This is in accordance with actual reality because, in actual practice, economic cost and carbon discharge have negative correlation. If the arranging department only puts focus on economic profits, it therefore will without question raise environmental pollution because of the increase in carbon discharge. On the opposite side, when merely environmental protection is got consideration, it can inevitably cause a rise of the total cost of electric power production.The Pareto solution sets give the scheduling department a very big number of scheduling choice options. The scheduler that we use may then carry out the selection of an appropriate scheduling solution on the basis of the actual existing circumstances. In this article, through the method of maximum satisfaction in numerous solution sets, we confirm that the optimal trade-off result of the two objective functions in the non-dominated solution set is the day-ahead unit and energy storage arrangement plan.

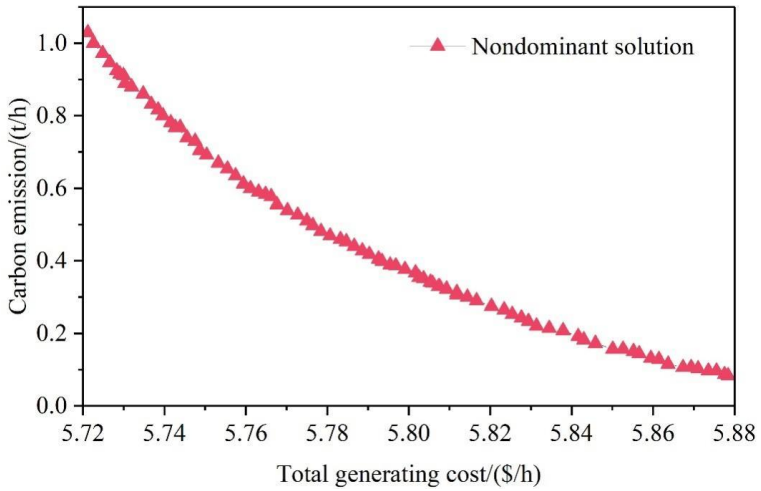

Figure 5: Pareto solution set frontier

The probability model of wind power generation imitates the size of wind power output in every time period. Figure 6 give depiction of its statistics probability distribution. Through the examination of the probability distribution graph, it is thus clearly seen that the wind power output has very great fluctuations. The output numerical values lie in the scope from zero to the rated power output of the wind energy system, hence most of the distribution is concentrated between 0 and 30 MW. This kind of mode extremely resembles the actual output which a wind farm produces.

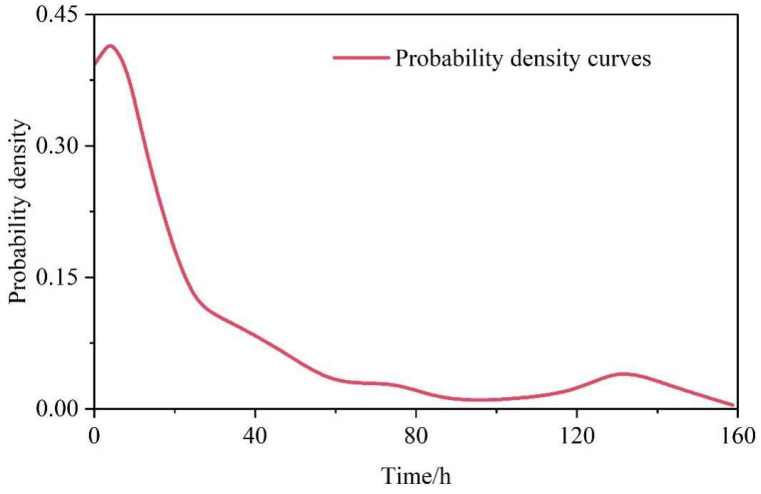

Figure 6: Probability distribution of wind power

For the difference between peak and trough, we have set a confidence level that is 0.99. By utilizing the method which is based on maximum satisfaction, the day-ahead arrangement scheme that corresponds to the optimized compromise resolution without energy storage participation is obtained, which is shown in Figure 7. At the same time, Figure 8 gives display of the day-ahead arrangement scheme under the situation that energy storage participates in.According to what Figure 7 shows, we can clearly see that when energy-storage does not take part in participation, many times of adjustment to the output of power-generating units is needed.In the early morning time period when the load has achieved its lowest value, the First Unit, the Second Unit, the Fourth Unit, and the Fifth Unit all work under a low power condition and have a high energy consumption. In addition, the maximum peak to trough difference in

the output of these units has a value of 262 MW.

According to what Figure 8 shows, after energy storage takes part in the unit scheduling interactions, the output of thermal power units becomes more steady. Under this circumstance, the units have not the situation that they undergo frequent starting and stopping processes. This not merely decreases the start and stop expenses of the units, but also alleviates the extra economic losses. In the time of early morning, when the electrical load is at a low level, the energy storage device is being in the condition of charging.In this moment, the energy storage works in a condition which is similar to a load. In comparison with the situation that energy storage does not take participation, the thermal power generating unit is able to keep its electric power producing condition, and it does not have the necessity for frequent starting and stopping. When the time comes to 21 o'clock, the load arrives at its highest point, the discharge power of the energy storage achieves its maximum value. This hereby contributes to the alleviation of the pressure which is borne by the unit in regard to peak regulation. When the cycle reaches its end, the electricity storage's charge state goes back to its starting value. The maximum charging ability of the energy storage inside the dispatch cycle appears near 4:00 a.m. Therefore, in the time periods when wind power attains the peak level, the charging process is undergone by the energy storage system. This greatly decreases the quantity of wind power cutting that is caused by the downstream pressure which is exerted upon the unit.

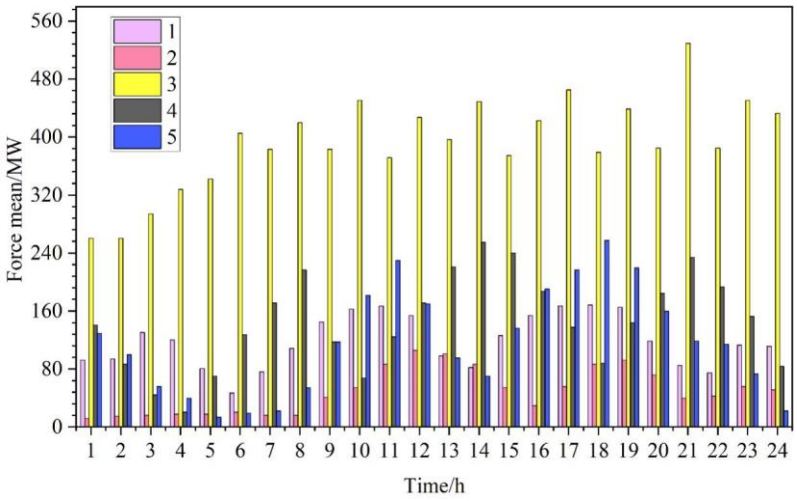

Figure 7: The output mean curve of the case1 unit

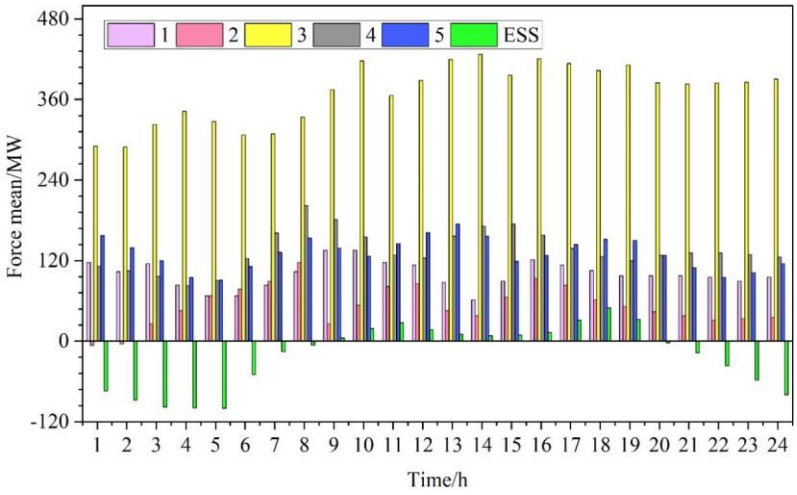

Figure 8: The output mean curve of the case2 unit

Table 7 gives the compare results about the effect of energy storage when scheduling on the target outcomes. A careful use of energy storage for carrying out unit arrangement, cooperating with the units to conduct load peak cutting and valley filling, therefore it can effectively reduce the energy expenditure and start-stop expenses of thermal power generating units. In addition, this method can decrease the carbon contamination discharge of heat electricity units, therefore it can thus obtain comparatively good environmental benefits. The multi-objective scheduling model that this paper puts forward can enable a quick and reasonable mutual action between energy storage systems and thermal power generating units. Through the utilization of energy storage in peak clipping and valley filling, more accommodation space can be provided by it for wind power. Furthermore, this method can obtain a 18.24% cut of carbon emissions, when it only makes the total cost of power generation have an increase of 9.56%. Along with the reduction of energy storage cost on the power grid side, energy storage is able to replace the traditional units which have high consumption and low efficiency in large-scale application scenarios that exist inside the electric power system.This substitution has the objective of making user electricity expenses as small as possible, making the system's net income as big as possible, and making the overall cost of electric power generation optimized, which includes the power peak adjustment cost inside the power supply cycle, and also the environmental protection costs.

Table 7: The schedule is compared to the target results

Situation	Mean cost of energy/$	The cost mean of the stop/$	The storage cost is the mean/$	The mean of the assembly/$	Mean of carbon emissions/t
No energy storage (case1)	1076522	2520	0	1079042	23.25
Energy storage (case2)	1043150	2355	136678	1182183	19.01

Table 8 gives a comparison research of the arrangement results under different confidence degrees of the peak-valley gap.When the confidence level α of the peak-valley difference becomes smaller, it can alleviate the situation that extreme wind power abandonment causes the rise of the net load peak-valley difference. Along with the proportion of wind electricity inside the system going up, there exists a comparatively small decline in both the total expenditure of coal-fired power equipment and carbon discharge amounts.This result further proves the reasonableness of adding the peak-valley gap opportunity restriction in this study. Therefore, in the dual-objective optimized dispatch model that this paper puts forward, which considers the stochastic chance restrictions of the peak-valley gap and the energy storage on power grid side, designers can reach the goal of energy saving and discharge reduction. They are able to complete this work through the setting of different confidence degrees in the risk scope that the electric power network can bear, according to the concrete planning demands.

Table 8: Different peak valley difference confidence level reduction results

Peak valley	0.99	0.97	0.95	0.93	0.91
Assembly mean/$	1182183	1151147	1131452	1112541	1102189
Mean of carbon emissions/t	19.01	18.87	18.44	18.07	17.78
Maximum acceptance of wind power/MW.h	770.55	895.45	1105.21	1315.44	1675.45

3.3 Evaluation of peaking optimization results

3.3.1 Peaking evaluation indicators

For the purpose of contrasting and evaluating the peak optimization results of the strategy which is put forward in this paper and the constant power strategy, the following evaluation indicators are given.

(1) Load absolute peak-to-valley difference ΔP_1.

$$\Delta P_1 = P_{\max} - P_{\min} \tag{30}$$

(2) Peak-to-peak coefficient.

Load valley wind coefficient α can indicate the degree of smoothness of the load curve, α the larger the value of the load curve fluctuation amplitude is smaller that is, the smoother.

$$\alpha = P_{\min} / P_{\max} \tag{31}$$

(3) Total wind abandonment.

$$P_{nw}^{t} = \begin{cases} P_{w}^{t} - P_{w,t}, & P_{w}^{t} > P_{w,t} \\ 0, & P_{w}^{t} \le P_{w,t} \end{cases} \tag{32}$$

Wind power abandonment occurs when the grid connected wind energy's output power exceeds the allowable power capacity that the system can hold.

3.3.2 Peaking optimization evaluation results

Figure 9 and Figure 10 separately give the comparison results before and after constant-power peak adjustment, and before and after peak adjustment by the strategy which this paper proposes.At the beginning, the combination of the virtual power plant into the electric network caused a quite obvious peak-valley difference. Nevertheless, when the energy storage system has completed the work of grid peak cutting and valley filling, this condition has thus seen a very big improvement.The problem of large load changes has already been effectively weakened. When we make comparison with the method of invariable power, the optimization strategy that we use in this place possesses a clear superiority. This work carries out an all-round evaluation of very many restriction factors. These elements include the energy storage device's volume, charge condition, and real-time system control management.On the opposite side, when the method of constant power is chosen, if the predicted occurrence and termination moments of load peak and load valley have deviation from the actual condition, a region in which peak regulation is still not finished will thus appear.

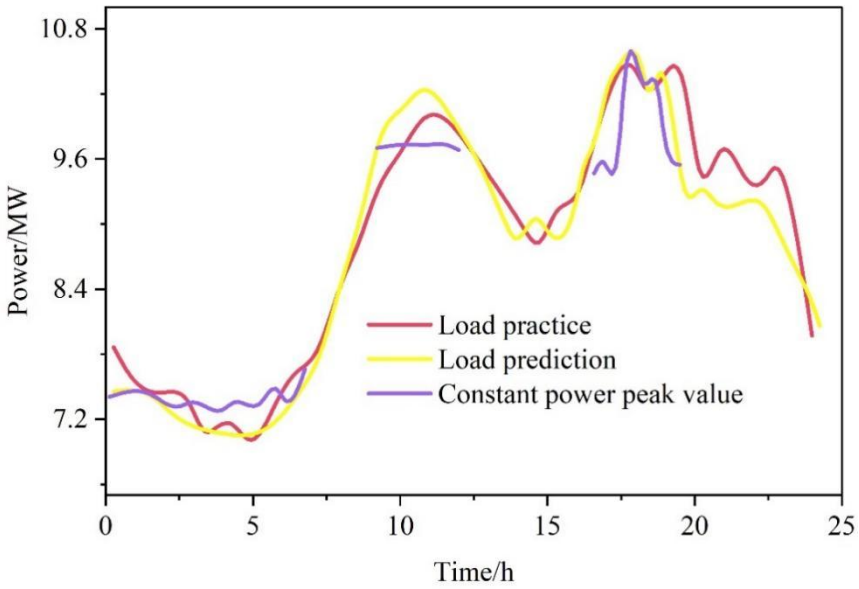

Figure 9: The constant power is compared to the peak

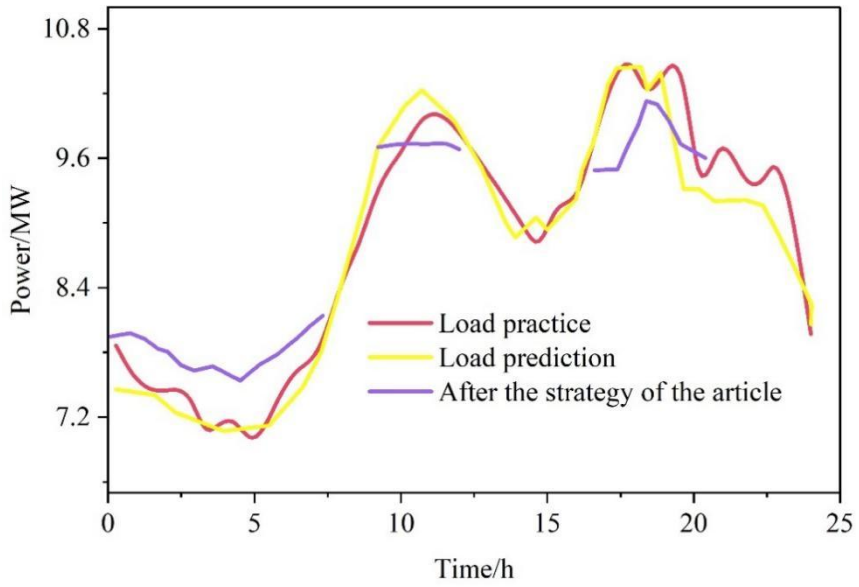

Figure 10: This paper strategies to compare and compare

Table 9 gives out the compare experiment results. After we separately carry out the strategy put forward by this paper and the constant-power peak adjustment, the disparity between load peak and load valley is obviously reduced, when it is compared with the condition that is before we conduct peak adjustment. Furthermore, the strategy that is proposed by this paper can bring more good effect. To speak specifically, when we compare it with the constant-power strategy, the peak-valley difference has a decrease of 320.3kW. The peak-to-valley coefficient acts as an indicator which reflects the severity of the fluctuation of the load factor.

After the peak adjustment of the strategy which this paper puts forward, the peak-to-peak coefficient becomes larger. When we carry out evaluation on the overall wind curtailment index, these two strategies do not have obvious difference. Therefore, these two kinds of strategies all have very high effectiveness in reaching the target of peak cutting and valley filling. The control tactic of the invariable-power method possesses a simple procedure. But, this method cannot take into consideration the real load changes that are inside the system. The energy storage

device makes its charge and discharge schemes according to the forecast load curve on every time point, and the charge and discharge power keeps unchanged.This strategy possesses obvious advantages and disadvantages. From the good aspect, the calculation procedure is not complex, and the execution way is comparatively near to actual world situations. However, this method possesses a comparatively big error range, particularly when it carries out real-time load cutting and peak filling control. Therefore, it requires a very high level matching between the real grid load and the load that is predicted. Therefore, hence, it only can be selectively used in the situations where the demands of control mode are not too complex, and the requirement for precision is not extremely high. When the real-world system load curve has divergence from the predicted load curve, the disadvantages of the fixed power control strategy become especially obvious. By contrast, the optimization method which is put forward in this paper can, according to the actual load on any specific time and any specific location, carry out adaptive adjustment on the electricity capacity of the energy storage system. This method has the function of preventing control failures and, therefore, thus promotes the degree to which the energy storage system makes contribution to grid peak cutting and valley filling.

Table 9: The experiment results

Optimization method	Prediction load	Actual load	Constant power	This strategy
Peak/KW	10564.1	10524	10425.2	10252.3
Valley value/KW	7032.5	69982	7432.2	7584.2
Absolute peak valley difference/KW	3532.1	3542	2992.8	2672.5
Peak valley coefficient	0.6658	0.6641	0.7125	0.7396
Wind power over/(kw*h)	1612.5	1598.2	1445.2	1460.3

4 Conclusion

Considering the problem that the net load peak-to-valley gap increases year by year because of new energy virtual power plants connected to the grid and the system’s peak adjustment capability is not enough, a multi-objective peak adjustment optimization model which considers the net load peak-to-valley difference is constructed. After that, the model is got solution through using a hierarchical particle swarm optimization algorithm. The main research achievement we get is these:

In this research work, a multi-objective optimized dispatch model has been constructed. Its aims are to make the customer's electricity spending as small as possible, make the system's net income as large as possible, and hence cut the power peaking cost in the whole power supply time period. This model may be utilized to arrange the charging of energy storage in time periods of low load and the discharging of energy storage in peak load time periods. Through adopting such method, it assists in the alleviation of pressure that lies on peak electric power demand. The model that we put forward obtains an environmental superiority, that is, a 18.24% cut of carbon discharge. This work is finished with only a 9.56% increment in the total electric power production cost. It can effectively reduce the whole system's total carbon discharge and working expenses. Furthermore, it provides a flexible decision-making space for the department that does scheduling work. According to the principles of economic efficiency and environmental protection, the optimal arrangement results of the multi-objective optimal arrangement model hold obvious scientific and economic properties. These characteristics possess advantages for facilitating the complete utilization of renewable energy sources and

enhancing the effect degree of energy consumption usage.

When we make comparison with the method of constant power, the strategy which is proposed in this paper possesses the capability to further reduce the difference between the peak and the valley of the net load. The disparity in the net load peak-to-valley numerical values between the two strategies reaches 320.3 kW. Both the strategy that this paper puts forward and the strategy of constant power can all have the contribution to the reduction of the peak-to-valley difference. However, the promotion that the strategy of this paper obtains is greatly more conspicuous. Furthermore, this strategy more accords with the actual operation features of the energy storage system. This alignment does not only assist to prolong the service life of the system but also brings about a further decreasing of the peaking cost.

About the Author

Zhenhai Zhu (1980.11.10-), male (Han ethnicity), native of Baoji, Shaanxi Province, holds a master's degree and is a senior engineer. Research focus: power systems.

Jiye Hu (1975.03.26-), male (Han ethnicity), native of Harbin, Heilongjiang Province, holds a Master's degree and is currently pursuing a Ph.D., specializing in engineering with a research focus on new energy systems.

Hui Sun (1982, 10, 27-), male (Han ethnicity), native of Yantai, Shandong Province, holds a bachelor's degree and is a senior economist. His research focus is on power systems. Yong Guo (born 25 July 1980), female (Han ethnicity), native of Chaozhou, Guangdong Province, holds a university degree and is a Senior Economist specializing in market transactions.

Lang Gan (1989.5.1-), male (Han ethnicity), native of Tianmen, Hubei Province, holds a bachelor's degree and is an engineer. His research focuses on power trading and virtual power plants.

Lei Yang (1995.8.28-), female (Han ethnicity), from Yichang, Hubei Province, holds a master's degree, Intermediate Economist, Research Focus: Power Trading, Virtual Power Plant.

References

[1] Babatunde, O. M., Munda, J. L., & Hamam, Y. (2019). A comprehensive state-of-the-art survey on power generation expansion planning with intermittent renewable energy source and energy storage. International Journal of Energy Research, 43(12), 6078-6107.

[2] Mlilo, N., Brown, J., & Ahfock, T. (2021). Impact of intermittent renewable energy generation penetration on the power system networks–A review. Technology and Economics of Smart Grids and Sustainable Energy, 6(1), 25.

[3] Auer, B. R. (2016). How does Germany's green energy policy affect electricity market volatility? An application of conditional autoregressive range models. Energy Policy, 98, 621-628.

[4] Li, C., Ding, G., He, L., & Cao, F. (2022, July). Peak-valley Time-of-Use Tariff Formulation Method Based on Net Load Curve. In 2022 IEEE/IAS Industrial and Commercial Power System Asia (I&CPS Asia) (pp. 1196-1201). IEEE.

[5] Guo, J., Xue, X., Li, L., Cheng, Y., & Li, Y. (2020, March). Peak-valley time division model based on net load curve. In IOP Conference Series: Earth and Environmental Science (Vol. 467, No. 1, p. 012037). IOP Publishing.

[6] Reihani, E., Motalleb, M., Ghorbani, R., & Saoud, L. S. (2016). Load peak shaving and power smoothing of a distribution grid with high renewable energy penetration. Renewable energy, 86, 1372-1379.

[7] Xiang, M., Zhang, Y., Li, C., & Qi, C. (2024). Peak-shaving cost of power system in the key scenarios of renewable energy development in China: Ningxia case study. Journal of Energy Storage, 91, 112133.

[8] Liang, J., Zhao, X., & Yang, S. (2021). Collaborative optimization model of renewable energy development considering peak shaving costs of various flexibility resources. Global Energy Interconnection, 4(4), 394-404.

[9] Jia, Y., Wang, Y., Bai, H., Wang, S., Li, Q., & Hua, Y. (2023, November). Electric vehicles participate in the economic optimal scheduling method of virtual power plant considering time-of-use tariff. In 2023 Power Electronics and Power System Conference (PEPSC) (pp. 266-275). IEEE.

[10] Zhang, F., Gong, Y., Zhang, X., Liu, F., & Zhou, Q. (2024). A multi-objective stochastic optimization model for combined heat and power virtual power plant considering carbon recycling and utilizing. Frontiers in Energy Research, 12, 1363360.

[11] Guo, W., Liu, P., & Shu, X. (2021). Optimal dispatching of electric-thermal interconnected virtual power plant considering market trading mechanism. Journal of cleaner production, 279, 123446.

[12] Chen, Y., Niu, Y., Du, M., & Wang, J. (2023). A two-stage robust optimization model for a virtual power plant considering responsiveness-based electric vehicle aggregation. Journal of Cleaner Production, 405, 136690.

[13] Michael, N. E., Hasan, S., Al-Durra, A., & Mishra, M. (2023). Economic scheduling of virtual power plant in day-ahead and real-time markets considering uncertainties in electrical parameters. Energy Reports, 9, 3837-3850.

[14] Elgamal, A. H., Shahrestani, M., & Vahdati, M. (2024). Assessing and comparing a DDPG model and GA optimization for a heat and power virtual power plant operating in a power purchase agreement scheme. Heliyon, 10(2).

[15] Ju, L., Lv, S., Zhang, Z., Li, G., Gan, W., & Fang, J. (2024). Data-driven two-stage robust optimization dispatching model and benefit allocation strategy for a novel virtual power plant considering carbon-green certificate equivalence conversion mechanism. Applied energy, 362, 122974.

[16] Rahimi, M., Ardakani, F. J., Olatujoye, O., & Ardakani, A. J. (2022). Two-stage interval scheduling of virtual power plant in day-ahead and real-time markets considering compressed air energy storage wind turbine. Journal of Energy Storage, 45, 103599.

[17] Cavazzini, G., Benato, A., Pavesi, G., & Ardizzon, G. (2021). Techno-economic benefits deriving from optimal scheduling of a Virtual Power Plant: Pumped hydro combined with wind farms. Journal of Energy Storage, 37, 102461.

[18] Tan, Y., Shen, Y., Yu, X., & Lu, X. (2023). Low-carbon economic dispatch of the

combined heat and power-virtual power plants: A improved deep reinforcement learning-based approach. IET renewable power generation, 17(4), 982-1007.

[19] Sharma, H., & Mishra, S. (2022). Optimization of solar grid-based virtual power plant using distributed energy resources customer adoption model: A case study of Indian power sector. Arabian journal for science and engineering, 47(3), 2943-2963.

[20] Zhao, H., Wang, X., Siqin, Z., Li, B., & Wang, Y. (2023). Two-stage optimal dispatching of multi-energy virtual power plants based on chance constraints and data-driven distributionally robust optimization considering carbon trading. Environmental Science and Pollution Research, 30(33), 79916-79936.

[21] Lee, S. J., Kim, J. H., Kim, C. H., Kim, S. K., Kim, E. S., Kim, D. U., ... & Khan, S. U. (2015). Coordinated control algorithm for distributed battery energy storage systems for mitigating voltage and frequency deviations. IEEE Transactions on Smart Grid, 7(3), 1713-1722.

[22] Ning, Y., Li, X., Ma, X., Jia, X., & Hui, D. (2016, June). Optimal schedule strategy of battery energy storage systems for peak load shifting based on interior point method. In 2016 12th World Congress on Intelligent Control and Automation (WCICA) (pp. 2285-2288). IEEE.

[23] Banshwar, A., Sharma, N. K., Sood, Y. R., & Shrivastava, R. (2017). Market based procurement of energy and ancillary services from Renewable Energy Sources in deregulated environment. Renewable Energy, 101, 1390-1400.

[24] Liu, S., Zhao, L., Huang, S., You, H., Li, J., & Yang, L. (2022). Research on the mixed control strategy of the battery energy storage considering frequency modulation, peak regulation, and SOC. Energy Science & Engineering, 10(9), 3459-3470.

[25] Badesa, L., Strbac, G., Magill, M., & Stojkovska, B. (2021). Ancillary services in Great Britain during the COVID-19 lockdown: A glimpse of the carbon-free future. Applied Energy, 285, 116500.

[26] Li, H., Sun, D., Li, B., Wang, X., Zhao, Y., Wei, M., & Dang, X. (2023). Collaborative optimization of VRB-PS hybrid energy storage system for large-scale wind power grid integration. Energy, 265, 126292.

[27] Heydari, R., Nikoukar, J., & Gandomkar, M. (2021). Optimal operation of virtual power plant with considering the demand response and electric vehicles. Journal of Electrical Engineering & Technology, 16(5), 2407-2419.

[28] Cui, Z., Chang, X., Xue, Y., Yi, Z., Li, Z., & Sun, H. (2024). Distributed peer-to-peer electricity-heat-carbon trading for multi-energy virtual power plants considering copula-CVaR theory and trading preference. International Journal of Electrical Power & Energy Systems, 162, 110231.

[29] Liu, J., Wang, H., Du, Y., Lu, Y., & Wang, Z. (2023). Multi-objective optimal peak load shaving strategy using coordinated scheduling of EVs and BESS with adoption of MORBHPSO. Journal of Energy Storage, 64, 107121.